Colloid Polym Sci (2005) 283: 711–720
DOI 10.1007/s00396-004-1207-z

M. Salmerón Sánchez
Y. Touzé
A. Saiter
J. M. Saiter
J. L. Gómez Ribelles

Influence of the chemical structure on the kinetics of the structural relaxation process of acrylate and methacrylate polymer networks

Received: 22 April 2004
Accepted: 27 August 2004
Published online: 20 October 2004

M. Salmerón Sánchez (✉) · Y. Touzé
J. L. Gómez Ribelles
Center for Biomaterials,
Universidad Politécnica de Valencia,
Camino de Vera s/n, 46022 Valencia, Spain
E-mail: masalsan@fis.upv.es
Tel.: +34-963877275
Fax: +34-963877276

Y. Touzé · A. Saiter · J. M. Saiter
Laboratoire d'Etude et Caractérisation des Amorphes et des Polymères,
Université de Rouen, Rouen, France

Abstract The enthalpy relaxation of poly(hydroxyethyl methacrylate) (PHEMA), poly(ethyl methacrylate) (PEMA) and poly(ethyl acrylate) (PEA) networks, obtained by DSC, are compared. The temperature interval of the glass transition broadens in the sequence PEA-PEMA-PHEMA. The plots of the enthalpy loss during the annealing for 200 min at different temperatures below T_g show that the structural relaxation process also takes place in PHEMA in a broader temperature interval than in PEA or PEMA. The modelling of the structural relaxation process using a phenomenological model allows determining the temperature dependence of the relaxation times concluding that the fragility in PHEMA is significantly lower than in PEMA. Both features are ascribed to the connectivity of the polymer chains in PHEMA via hydrogen bonding. The role of the presence of the methyl group bonded to the main chain is analysed by comparing the results obtained in PEA and PEMA.

Keywords Structural relaxation · Glass transition · DSC · PEA · PEMA · PHEMA

Introduction

The structural relaxation is the process of approaching an equilibrium state by a glass held at constant temperature and pressure after its formation history [1, 2]. Several physical magnitudes—such as enthalpy, volume or entropy—are higher in the so-called glassy state than in the equilibrium state, at the same temperature and pressure, and tend to the equilibrium values during the relaxation process.

Differential scanning calorimetry (DSC) is a useful technique in the study of the kinetics of the structural relaxation process. The experimental thermograms can be exploited by means of the calculation of the enthalpy relaxation (at different annealing temperatures and times) and also through the use of phenomenological models with fitting parameters [3–9]. Anyway, the sample is subjected to a thermal history starting at a temperature T_0 higher than its glass transition temperature; after cooling at a controlled rate to a temperature T_a below, or in the region of, the glass transition, the sample is kept isothermally for a period of time t_a. The material is then brought at a fixed cooling rate to a temperature T_1 below T_g, and subsequently heated from T_1 to T_0. The last heating thermogram shows a characteristic peak of the specific heat capacity that depends very sensitively on the previous thermal history, i.e., the annealing temperature T_a and time t_a (Fig. 1). It can be shown that the enthalpy loss in the sample during the isothermal stage at T_a is equal to the area (from T_1 to T_0) between the heating thermogram measured immediately after the annealing process, c_p, and that deter-

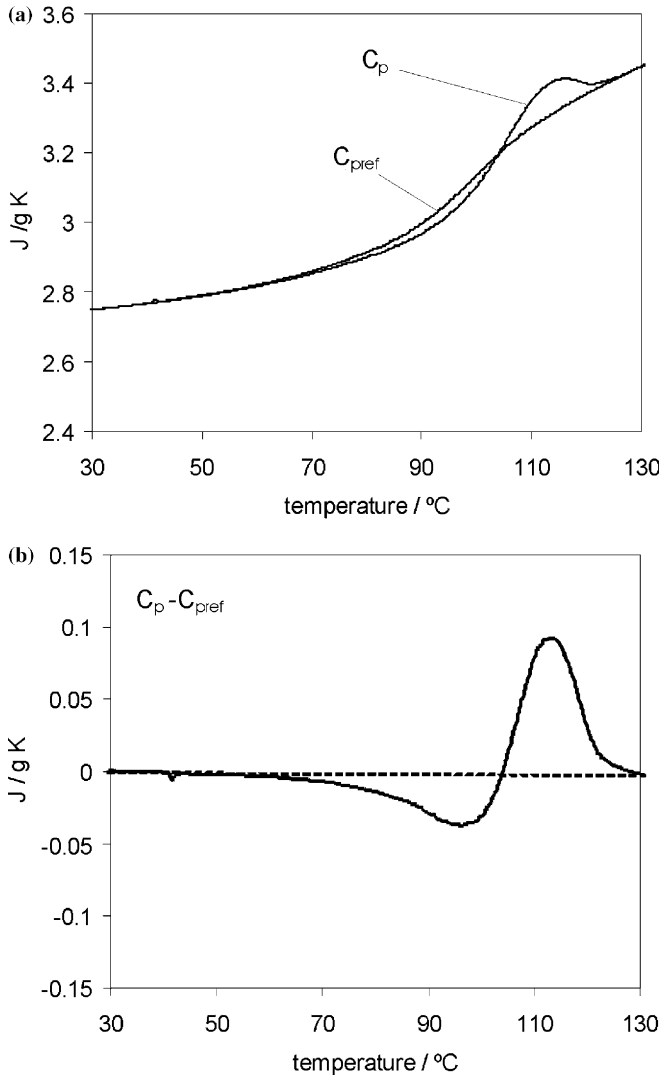

Fig. 1 **a** Temperature dependence of the heat capacity of a PHEMA network subjected to an annealing process c_p at a temperature T_a (80 °C) below T_g showing the characteristic peak. The unannealed reference scan, c_{pref} is also included. **b** The $c_p - c_{pref}$ curve obtained on subtracting the annealed and unannealed curves

mined between the same temperatures in a scan without annealing, c_{pref}, the reference scan [10, 11],

$$\Delta H(T_a, t_a) = \int_{T_1}^{T_0} \left(c_p(\theta) - c_{pref}(\theta)\right) d\theta. \quad (1)$$

Figure 1 shows an example of the DSC thermograms and the curve obtained after subtracting the reference scan from the annealed curve.

The structural relaxation process reveals the existence of conformational motions in the glassy state whose kinetics depends on the chemical structure of the material. The information obtained from DSC scans after the above-described thermal history can be quantified by the use of mathematical models with fitting parameters. These parameters must depend only on the nature of the material under study and not on the thermal history used in the fitting procedure [8–9]. In this sense, the set of parameters obtained after a fitting of the experimental data to the model allows not only the prediction of the thermograms for thermal histories not included in the fitting analysis, but also a set of values that characterises the dynamical properties of the material. This fact can be used for studying the influence of some chemical groups in the dynamics of the system, i.e. in the process of approaching to equilibrium from the glassy state. The differences found between the poly(ethyl acrylate) (PEA) and poly(ethyl methacrylate) (PEMA) networks can be ascribed to the presence of the methyl group in the second one. On the other hand, what distinguish the poly(hydroxyethyl methacrylate) (PHEMA) and PEMA networks are the hydroxyl groups, and the possibility of hydrogen bond formation, in the former. The comparison among the kinetics of the process in these three systems, as revealed by the used of a phenomenological model, gives information on the influence of the methyl group and the hydroxyl group on the relaxation process.

In this work, we have used the SC model [8, 9] that follows the evolution of the configurational entropy S_c during the structural relaxation process. The SC model has already been used successfully in the study of the process in several polymer systems [8, 9, 12–16] and its use has shown some advantages with respect to phenomenological models that tackle the same problem [17]. The model is a modification of that of Scherer–Hodge [3, 7] but using S_c instead of the fictive temperature and where the equations are presented in such a way that the limit of the isothermal structural relaxation, S_c^{lim}, can be assumed to be different from the equilibrium states obtained by extrapolation from the experimental values measured at temperatures above T_g, S_c^{eq}.

The SC model assumes that for a given thermal history up to a time t, $T(\sigma)$, $-\infty \leq \sigma \leq t$, the configurational entropy S_c depends on a 'quasilinear' form of the thermal history when expressed in a reduced time

$$\hat{u}(t) = \int_0^t \frac{d\xi}{\tau(\xi)}, \quad (2)$$

where τ is a relaxation time that will be defined below, so

$$S_c(t) = S_c^{lim}(T(t)) - \int_0^{\hat{u}(t)} \phi(\hat{u}(t) - u) dS_c^{lim}\left(\tilde{T}(u)\right). \quad (3)$$

ϕ is a relaxation function of the Kohlrausch–Williams–Watts (KWW) type [18]

$$\phi(u) = \exp\left(-u^{\beta}\right) \tag{4}$$

and $\tilde{T}(u)$ is the temperature history expressed in the new time scale (Eq. 2).

In Eq. 2, it is assumed for τ a dependence on the instantaneous values of configurational entropy and temperature as an extension of the Adam and Gibbs [19] expression for nonequilibrium states

$$\tau(S_c, T) = A \exp\left(\frac{B}{S_c T}\right). \tag{5}$$

When the configurational entropy S_c has the equilibrium values S_c^{eq} (T), Eq. 5 remains the same for the dependence of the equilibrium relaxation times on temperature, but the equation

$$S_c^{eq}(T) = \int_{T_2}^{T} \frac{\Delta c_p(\theta)}{\theta} d\theta \tag{6}$$

is now valid. In this last equation, T_2 is the Gibbs–Di-Marzio transition temperature [20], $\Delta c_p(T) = c_{pl}(T) - c_{pg}(T)$, the difference between the heat capacity in the liquid and glassy state, is the configurational heat capacity.

It has been proved that in many polymers the fit to the experimental results is improved when S_c^{lim} is significantly higher than S_c^{eq} . When this is assumed,

$$\frac{dS_c^{lim}}{dT} = \frac{\Delta c_p - \delta}{T}, \tag{7}$$

where δ is a fitting parameter ($\delta = 0$ reflects the assumption of an equilibrium limit state) that represents the impossibility of conformational rearrangements to take place when the number of configurations available to the polymer segments attain a certain limit due to steric constraints, i.e. perfect packing of the chains in an amorphous glass can rarely be achieved. A sketch of the physical meaning of the δ parameter is shown in Fig. 2. The details of the calculation procedure and the fitting routines have been explained elsewhere [8, 9].

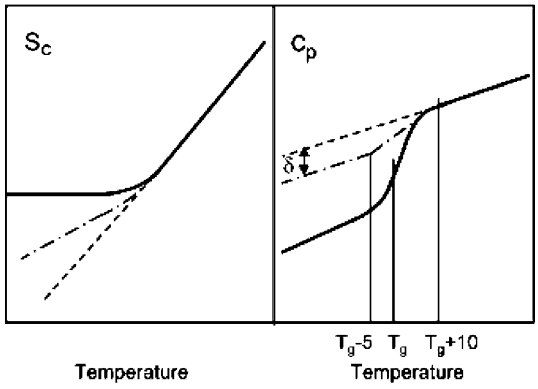

Fig. 2 **a** Sketch of the configurational entropy corresponding to the liquid state (*dashed line*), to an experimental cooling scan at a finite cooling rate (*solid line*), and to the hypothetical line of the limit states of the structural relaxation process (*dashed-dotted line*). **b** $c_p(T)$ lines corresponding to the three cases described in **a**: the *dashed line* corresponds to the liquid state $c_{pl}(T)$, the *solid line* corresponds to an experimental cooling scan and the *dashed-dotted line* corresponds to the specific heat capacity in the limit states of the structural relaxation process $c_p^{lim}(T)$. The fitting parameter δ shown in the figure characterizes the difference between the slopes of the $S_c^{eq}(T)$ and $S_c^{lim}(T)$ lines below the glass transition

Experimental methods

Polymer networks PEMA, PHEMA and PEA (monomers from Aldrich 99% pure) were polymerised via ultraviolet light using ethyleneglycol dimethacrylate (EGDMA; Aldrich, 98% pure) as crosslinking agent (2% weight) and benzoine (Scharlau 98% pure) as photoinitiator (0.13% weight). Low molecular weight substances were extracted from the polymer network by boiling in ethanol for 24 h and then drying it in vacuo at a temperature 20 °C above T_g to a constant weight. Stoichiometry allows us to calculate the average number of monomeric units between network junctions taking into account the molecular mass of each one of the monomeric units and the tetrafunctionality of the crosslinker: 45 (PEA), 41 (PEMA) and 37 (PHEMA).

Differential scanning calorimetry was performed in a Pyris 1 apparatus (Perkin Elmer). Dry nitrogen gas was let through the DSC cell with a flow rate of 20 ml/min. The temperature of the equipment was calibrated by using water and indium. The heat of fusion of indium was used for calibrating the heat flow. The sample was subjected to a thermal history that started at 150 °C for the PHEMA and PEMA networks, and at 70 °C for the PEA network. The sample was then cooled at 40 °C/min to the annealing temperature T_a, kept isothermally for different times ranging from 50 to 1000 min, and cooled again at 40 °C/min to −40 °C. Besides, the sample was subjected to cooling scans from the equilibrium temperature to −40 °C at different rates. In all cases, the subsequent heating scan from this temperature to the starting one took place at 10 °C/min. Immediately after each of these experiments, a heating reference scan at 10 °C/min was performed after cooling the sample from the highest to the lowest temperature, from T_0 to T_1, at 40 °C/min. In this way, the baseline of the DSC corresponding to the annealing and the reference scans is nearly identical and the position of the sample in the sample holder of the DSC is the same as well. The difference between both scans is zero with great accuracy at the start and the end of the thermogram. The normalized heat flow, which has heat capacity units, is obtained by dividing the heat flow as obtained from the apparatus by the mass and the heating rate, and was employed

instead of the absolute value of the specific heat capacity.

Results and discussion

The glass transition temperature of the three systems studied, as determined from the crossing point of the enthalpy lines corresponding to the liquid and the glassy states, is displayed in Table 1. Compared to the simplest network, the acrylate PEA, the PEMA presents an extra methyl group responsible for the dramatic increases in T_g. On the other hand, the presence of the hydroxyl group in the PHEMA provokes still a higher T_g but a lower change relative to that found in the PEMA network. At the same time that the glass transition shifts to higher temperatures, the temperature interval of the transition broadens. The width of the glass transition can be characterized by ΔT_g, the temperature difference between the crossing point of the tangent to the thermogram in the inflexion point of the transition with the liquid and the glass lines, respectively (the values of ΔT_g for the three samples are also shown in Table 1).

The differences found in the glass transition when changing the chemical structure of the monomeric unit is a consequence of the difference in the kinetics of the cooperative conformational rearrangements of the polymer chains, i.e. of the structural relaxation process. The glass transition temperature or even the width of the temperature interval in which it takes place are a poor characterization of the structural relaxation process, the values of T_g and ΔT_g are unable to explain the kinetics of this process. The DSC experiments that include isothermal annealing at different temperatures and times are needed for understanding the process and a deeper study of the influence of the different chemical structures on its kinetics.

Experimental thermograms were measured after relaxation experiments of 200 min at different temperatures (every 5 °C starting well below the glass transition and up to 10 °C above T_g). After each thermal history, a heating thermogram was recorded and then a reference scan followed with no change of the position of the sample and reference pans in the DSC holder. The difference between these two thermograms equals the difference between the heat capacity in the annealed and the reference scans ($c_p - c_{pref}$). Figure 3 shows the magnitude obtained for the PEMA network and similar figures can be plotted for the other two networks. In any case, the magnitude of the peaks, which depends on the annealing temperature, tends to vanish both at temperatures sufficiently higher and lower than T_g and allow us to identify the temperature range, where conformational motions take place in the material. From the area defined by the ($c_p - c_{pref}$) curves, a measure of the enthalpy loss during the structural relaxation process is obtained that it has been plotted, as a function of the annealing temperature, in Fig. 4a for the three networks. This figure suggests that the temperature interval, where conformational motions take place in the PEA network, is narrow with a well defined maximum when the annealing temperature is around −20 °C (around 8 °C below the enthalpic T_g) and it continues almost until −40 °C, i.e. 25 °C below T_g. The phenomenology of the structural relaxation process in the case of the methacrylate networks is different. In both cases (PEMA and PHEMA), the maximum is located around 15 °C below T_g but conformational motions are detectable at temperatures even 60 °C below T_g as the long tail in the ($c_p - c_{pref}$) curve reveals (Fig. 3a). On the other hand, the peak shown in Fig. 4a is higher in the acrylate network than in the methacrylate for which it is almost the same. Since the value of the enthalpy loss is proportional to the number of monomeric units participating in the relaxation process at T_a, the height and the width of the curve are related to each other. This can be better seen if the enthalpy loss is plotted versus $T_g - T_a$ as it has been done

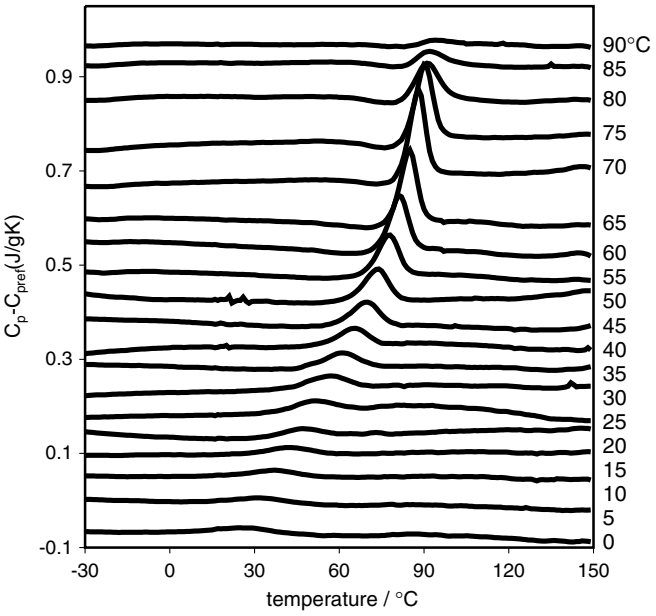

Fig. 3 Temperature dependence of $c_p - c_{pref}$ calculated for PEMA network from the thermograms measured after annealing for 200 min at the temperature shown in the graph. The curves have been vertically shifted for clarity

Table 1 Parameters at the glass transition region for the three networks

Network	T_g (°C)	ΔT_g	$T_{g\tau=100\ s}$ (°C)	$\Delta c_p(T_g)$ (J/gK)
PHEMA	99	18	103.8	0.31
PEMA	81	8	82.8	0.26
PEA	−8	3.5	−8.5	0.46

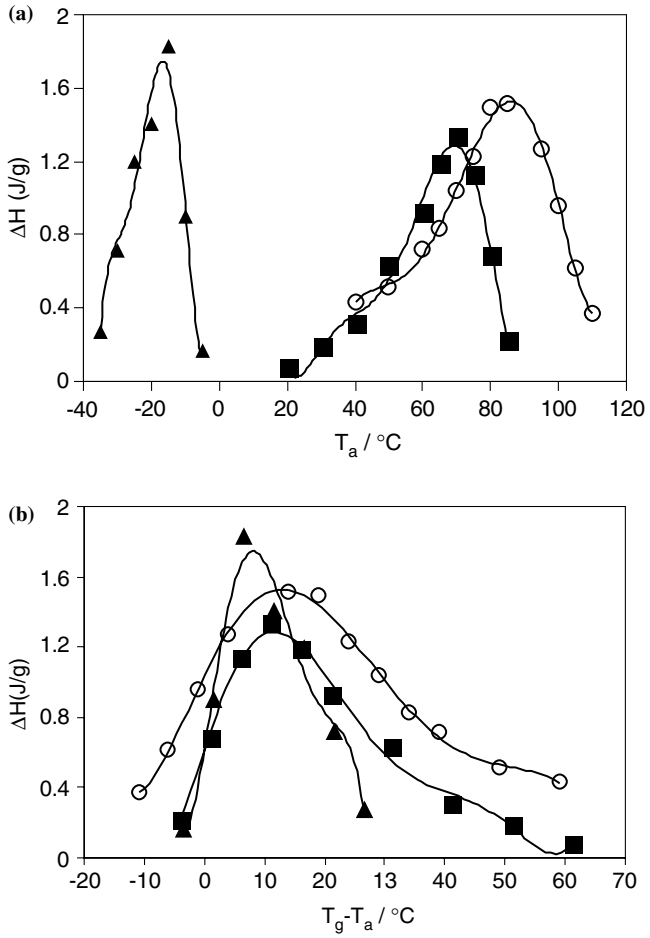

Fig. 4 Enthalpy loss during the isothermal annealing for the PHEMA (*open circle*), PEMA (*filled square*), and PEA (*filled triangle*) networks. **a** Versus annealing temperature. **b** Versus the normalized annealing temperature taking into account T_g. Curves between points are a guide to eye

in Fig. 4b. A broad glass transition interval reflects the presence of T_g fluctuations in the material and only a part of the polymer segments participate in the structural relaxation process at each temperature. (The T_g fluctuations may have different origins in different glass-forming materials. They can be originated by free volume fluctuations, inhomogeneous distributions of the network junctions, composition fluctuations in multicomponent systems, etc.). The more homogenous the system is, the higher and narrower are the peaks in the enthalpy loss curve. Since the glass transition temperature falls within the temperature interval in which the glass transition—the departure from the equilibrium when the sample is cooled from high temperatures—takes place a few degrees above T_g and, as a consequence, structural relaxation is detected at temperatures above T_g or for $T_g - T_a < 0$. This broader the glass transition is the more clear this feature becomes. This is the reason why the three curves in Fig. 4b do not merge for low values of $T_g - T_a$. The curves in Fig. 4 characterize in some ways the temperature interval in which cooperative conformational rearrangements take place in a time in the order of the annealing time, i.e. 200 min. This temperature interval is broader in the methacrylate networks than in PEA and especially in PHEMA (a way of characterizing the width of the enthalpy loss curves is by the temperature interval at half the height of the maximum: 20 °C, PEA; 30 °C, PEMA; 40 °C, PHEMA). This fact is parallel to the increase of ΔT_g in the sequence PEA-PEMA-PHEMA. A deeper insight in the kinetics of the process can be achieved by the use of the SC model. The experimental thermograms are obtained after 33 different thermal histories with different values of T_a and t_a. Figures 5, 6 and 7 show several curves measured after different thermal histories for the PHEMA, PEMA and PEA networks, respectively.

According to the theory that yields the model equations a single set of five model parameters (A, B and T_2 that determines the temperature dependence of the relaxation times in equilibrium, β, the KWW parameter, and δ that characterizes the limit states of the process) must characterize the kinetics of the structural relaxation for a given material, and consequently the model equations with this single set of parameters must reproduce the experimental thermograms measured after any thermal history. The uncertainty in the determination of the set of model parameters depends on the amount of experimental information introduced in the fitting routine, i.e. the number of experimental

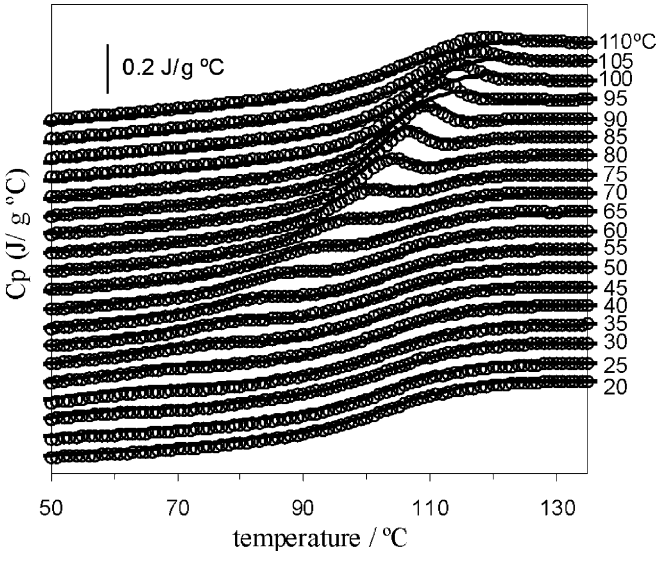

Fig. 5 Experimental normalized heat flows measured for the PHEMA network in heating scans after thermal histories that include an isothermal annealing during 200 min at the temperature specified in the graph. The *continuous line* represents the prediction of the model for the parameters shown in Table 1 ($B = 1000$ J/g)

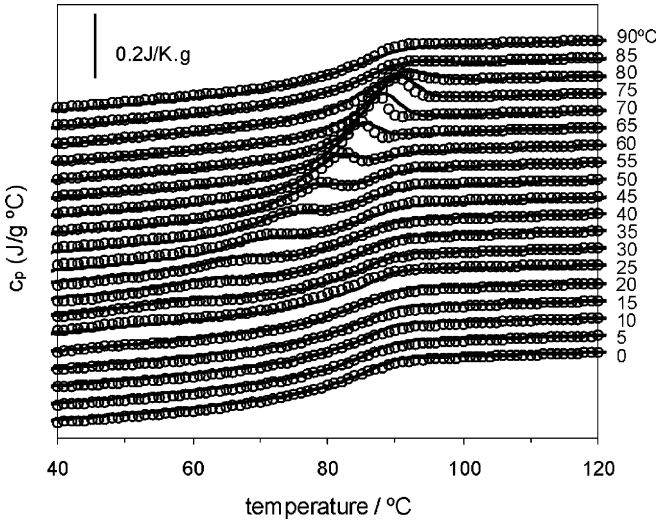

Fig. 6 Experimental normalized heat flows measured for the PEMA in heating scans after thermal histories that include an isothermal annealing during 200 min at the temperature specified in the graph. The *continuous line* represents the prediction of the model for the parameters shown in Table 2 ($B = 500$ J/g)

thermograms that are fitted simultaneously. The fits to a single thermogram yield very different sets of parameters depending on the thermal history selected, but if the number of thermograms increases, and the model equations actually reproduce the material behaviour, the set of parameters determined must become independent on the set of thermal histories used [21].

In this work, for a fixed number of experimental thermograms the fitting procedure was conducted for 15 different combinations of n files chosen among the available thermal treatments. This allows calculating the average value of each one of the model parameters and its standard deviation. The correlation existing between the parameters B, T_2 and ln A, similar to that observed for other phenomenological models such as those of Narayanaswamy–Moynihan or Scherer–Hodge [3, 5, 7], led us to fix the value of B and determine the other parameters with the least-squares routine. Figure 8 shows the evolution of the uncertainty (standard deviation) of model parameters as a function of the number n of experimental thermograms simultaneously used in the fitting process obtained with a fixed value of $B = 500$ J/g for PHEMA network. It is clearly observed that the standard deviation reduces as the number of files simultaneously fitted increases and it reaches an almost constant value for n higher than 7. From this analysis, it was decided to simultaneously fit eight thermograms each time. It must be mentioned here that the uncertainty obtained in each one of the parameters must be understood in their context: the model prediction is sensitive to such a change in the values of the parameters. In this sense, a variation in the value of the parameters of the order of the uncertainty produces a significant change in the quality of the fitting.

Tables 2, 3 and 4 show the values of the model parameters for different values of B. Several model parameters depend only slightly on the value of B fixed in the search routine. The value of δ is nearly

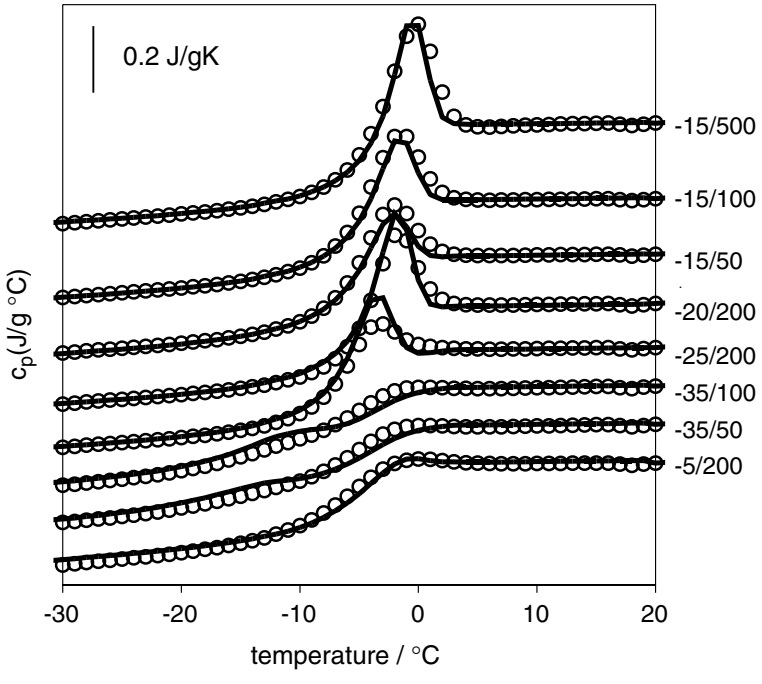

Fig. 7 Experimental normalized heat flows measured for the PEA in heating scans after different thermal histories specified in the graph [T_a(°C)/t_a (min)]. The *continuous line* represents the prediction of the model for the parameters shown in Table 3 ($B = 900$ J/g)

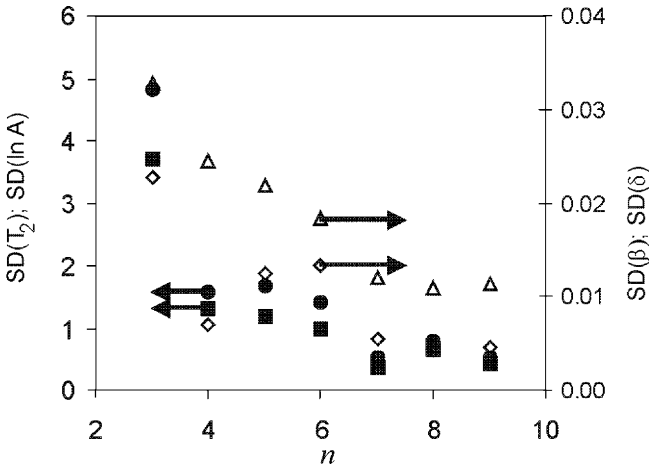

Fig. 8 Standard deviation of the model parameters as a function of the number n of thermal histories simultaneously used in the fitting procedure for the PHEMA network using $B = 500$ J/g. Each point is the average value of 15 fittings with different n files chosen among 33 thermal histories. T_2 (*filled square*), ln A (*filled circle*), β (*open triangle*), δ (*open diamond*)

Table 2 Model parameters found for the PHEMA network for each value of the parameter B

B (J/g)	δ (J/gK)	β	T_2 (°C)	ln A
500	0.111 ± 0.005	0.230 ± 0.012	57.0 ± 2.0	−24.20 ± 1.5
600	0.103 ± 0.010	0.238 ± 0.004	52.2 ± 0.7	−26.16 ± 0.6
700	0.121 ± 0.014	0.228 ± 0.021	48.6 ± 1.6	−28.33 ± 1.3
800	0.107 ± 0.010	0.231 ± 0.011	44.5 ± 1.0	−29.85 ± 0.9
900	0.114 ± 0.012	0.233 ± 0.006	40.7 ± 1.0	−31.22 ± 0.9
1,000	0.095 ± 0.013	0.243 ± 0.007	36.9 ± 1.1	−32.49 ± 1.0
1,100	0.113 ± 0.024	0.235 ± 0.009	33.9 ± 1.8	−33.89 ± 1.5

The standard deviation for each parameter is included

independent of B in any network, the highest value is found for the PEA network and the lowest for the PEMA. However, when the value is compared with the heat capacity increment at T_g (Table 1), a proportion of around 40% is found independently of the chemical structure. This fact suggests that the chemical character of the network does not have an influence on the limit state attained by the material after the structural relaxation process, quite far from the extrapolated equilibrium in any case.

Table 3 Model parameters found for the PEMA network for each value of the parameter B

B (J/g)	δ (J/gK)	β	T_2 (°C)	ln A
300	0.086 ± 0.013	0.282 ± 0.008	48.2 ± 1.1	−25.5 ± 1.2
400	0.089 ± 0.011	0.282 ± 0.008	42.9 ± 1.1	−29.5 ± 1.0
450	0.086 ± 0.012	0.288 ± 0.006	41.3 ± 1.3	−31.9 ± 1.3
500	0.083 ± 0.020	0.286 ± 0.008	38.5 ± 0.7	−32.8 ± 0.7
600	0.076 ± 0.016	0.290 ± 0.007	34.4 ± 1.2	−35.9 ± 1.1
700	0.081 ± 0.027	0.293 ± 0.009	30.2 ± 0.8	−37.9 ± 0.7

The standard deviation for each parameter is included

Table 4 Model parameters found for the PEA network for each value of the parameter B

B (J/g)	δ (J/gK)	β	T_2 (°C)	ln A
700	0.182 ± 0.005	0.398 ± 0.007	−48.3 ± 0.7	−28.33 ± 0.54
800	0.173 ± 0.099	0.399 ± 0.010	−50.1 ± 0.9	−30.12 ± 0.84
900	0.185 ± 0.026	0.405 ± 0.024	−52.4 ± 1.7	−32.58 ± 1.41
1,000	0.175 ± 0.011	0.400 ± 0.005	−54.2 ± 0.6	−34.64 ± 0.53

The standard deviation for each parameter is included

The value of β that characterizes the shape of the relaxation function depends only slightly on the value of B selected. The lower β is, the higher the width of the distribution of relaxation times. β is higher in the PEA network than in the methacrylate. The very small values of β in poly(alkyl methacrylates) were already reported in the literature [2, 3, 9, 22]. When comparing PHEMA and PEMA networks, the presence of the hydroxyl group seems to suggest a wider relaxation function ϕ, what is well correlated with the broad curve obtained for the PHEMA network in Fig. 4, when the enthalpy loss at each annealing temperature was calculated.

On the other hand, the parameters T_2 and ln A clearly correlate with B both in the acrylate and methacrylate networks, as found in many other systems [2, 8–17]. When B increases, both T_2 and ln A decrease. Mathematically this means a *scenario* where a 5-dimension hyper-surface shows several minima: different values of the model parameters are able to reproduce the experimental thermograms with almost the same accuracy. Some physical arguments can be used in order to delimitate the more appropriate range of B values. These could rely either on assuming the universality of the relationship between T_2 and T_g in polymeric materials [19, 23], but this argument would yield the same fragility for all polymer systems what is unrealistic. The results from other experimental techniques (viscoelastic or dielectric experiments) can be used to determine independently one of the model parameters, T_2 or B. The comparison between the model parameters of the different polymers can be also done on the basis of a value for the preexponential factor A equal to 10^{-14} s, i.e. ln $A = -32.2$, which is the value frequently ascribed to the limit of the relaxation time at high temperature [24]. The latter is the procedure followed in this work that yields a value of B of 900, 450 and 1000 J/g for PEA, PEMA and PHEMA, respectively. The values of the model parameters under this assumption for the three networks are summarised in Table 5.

Once the value of B has been chosen, the 33 thermograms measured after different thermal histories can be reproduced with the same set of parameters. Some of the theoretical curves predicted by the model for some of the thermal histories have also been included in Figs. 5,

Table 5 Model parameters selected, activation energies and fragility for the PHEMA, PEMA and PEA networks

Network	B (J/g)	β	T_2 (°C)	$T_g - T_2$ (°C)	S^c_{eq} (T_g) (J/g °C)	S^c_g (J/g °C)	m^a	$\Delta h^{*a}/R$ (kK)	m^b	$\Delta h^{*b}/R$ (kK)
PHEMA	1,000	0.243	36.9	62.1	0.070	0.056	84	70	112	96
PEMA	500	0.286	38.5	42.5	0.036	0.025	126	101	127	104
PEA	900	0.405	−52.4	44.9	0.090	0.084	100	61	123	75

[a]Values obtained using the model
[b]Experiments at different cooling rates

6 and 7 for each one of the networks. The agreement between the experimental results and the theoretical predictions is excellent for the methacrylates and quite good for the PEA. It is noteworthy how the model is able to predict, with the same set of parameters, curves phenomenologically so different as the characteristic prepeak at the low-temperature side of the glass transition when the treatment is performed at low temperatures [25–28] and those with a single and high annealing peak (see Figs. 5, 6, 7).

It is noteworthy that the shape of the thermograms measured after annealing of PHEMA at the highest temperatures from $T_a = 95$ °C up, the peak shown by the thermogram seems to be the result of the overlapping of two peaks. This shape can be the result of the existence in the material of some domains with higher glass transition temperature than the average. The model predicts obviously a single peak that appears in the position of the low-temperature shoulder of these thermograms and corresponds to the enthalpy recovery of those domains of the material with the lower T_g. The high-temperature peak shown by the samples annealed at high temperatures could be due to micelles formed in PHEMA by intra- or inter-chain hydrogen bonding. The conformational mobility of these micelles would be greatly reduced with respect to the rest of the material. This feature is not shown by PEA or by PEMA networks.

The three parameters B, A and T_2 determine the curve of the equilibrium relaxation times (Eqs. 5, 6).

$$\tau^{eq}(T) = A \exp\left(\frac{B}{T \int_{T_2}^{T} \frac{\Delta c_p(\theta)}{\theta} d\theta}\right). \tag{8}$$

Hence, as the different sets of parameters are able to reproduce the experimental thermograms with almost the same accuracy, the curves of the temperature dependence of the equilibrium relaxation times determined with a different set of parameters are almost coincident due to the correlation among B, A and T_2 (results not shown). The possibility of having the same $\tau^{eq}(T)$ dependence with different values of the model parameters is the physical reason why different sets of parameters determine almost the same experimental thermogram [9, 12].

Figure 9 shows for the three polymers the model-simulated temperature dependence of the relaxation time for a heating ramp calculated after cooling at 40 °C/min from equilibrium, i.e. for the reference scan. The glass transition temperature used to normalize this plot was the temperature at which the relaxation time in equilibrium equals 100 s, $T_{g\tau=100}$ (Table 1).

At low temperatures, in the glassy state, a linear dependence of ln τ with reciprocal temperature is found, according to a constant apparent activation energy

$$\frac{\Delta h^g}{R} = \left.\frac{d \ln \tau}{d 1/T}\right|_{glass} \tag{9}$$

that can be deduced from Eq. 5 since the configurational entropy in the glassy state is nearly constant, S_c^g .

$$\frac{B}{S_c^g} = \left.\frac{d \ln \tau}{d 1/T}\right|_{glass} \tag{10}$$

Table 5 shows the values of S_c^g calculated from Eq. 10 and the values of the configurational entropy in equilibrium at the glass transition temperature $T_{g\tau=100}$, S_c^{eq} (T_g). The values of S_c^g and S_c^{eq} (T_g) are close to each other in the case of a narrow glass transition since the configurational entropy in a cooling scan frozen suddenly close to its equilibrium value. In the case of a broad glass transition interval, S_c^g can be significantly smaller than S_c^{eq} (T_g) as happens in the PEMA and PHEMA networks.

At high temperatures, above the glass transition, the plot shows the characteristic trend of the Vogel equation, predicted by Eq. 8. At each temperature above the glass transition, conformational motions are slower in the PHEMA network than both the PEA and PEMA for which the equilibrium relaxation times are quite similar. This result seems to suggest that the interchain hydrogen bonds, due to the presence of the hydroxyl group in the PHEMA network, makes the dynamics of the system slower. This feature can be discussed in terms of the so-called dynamic fragility [24]. The difference $T_g - T_2$ is much higher in PHEMA than in PEA or PEMA (Table 5) indicating that the former has a stronger dynamic behaviour. The fragility parameter m is defined by

$$m = \left.\frac{d \log \tau^{eq}}{d T_g/T}\right|_{T_g}. \tag{11}$$

The calculated values for the three systems are shown in Table 5. The PHEMA network seems to be *stronger*

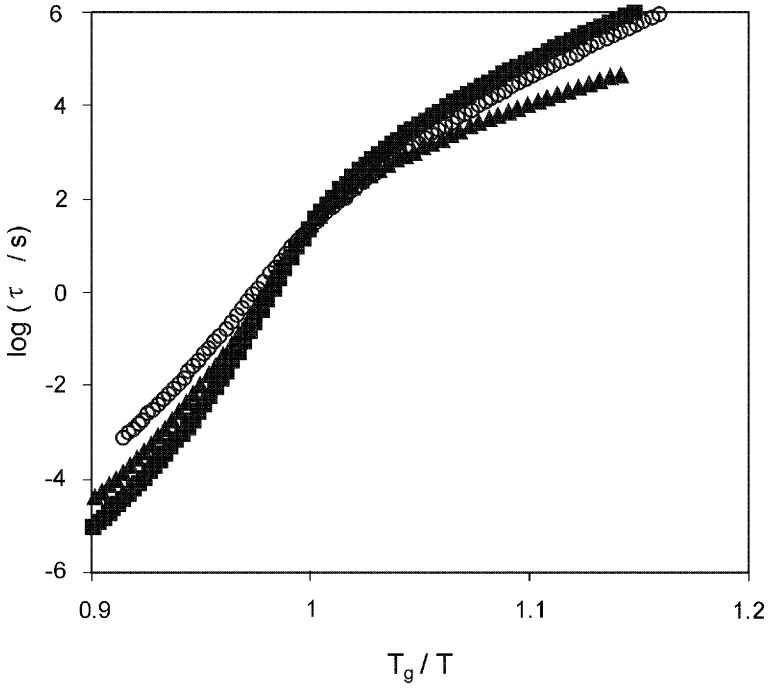

Fig. 9 Relaxation times determined by the model simulation of a heating scan carried out after cooling the sample at 40 °C/min from the equilibrium liquid for the PHEMA (*open circle*), PEMA (*filled square*) and PEA (*filled triangle*) networks. The model parameters are shown in Table 5

than both the PEMA and PEA as is qualitatively shown in the fragility plot (Fig. 9). However, the fragility parameter can also be obtained from the experimental heating thermograms measured after cooling the sample at different cooling rates, ranging between 0.5 and 40 °C/min, according to the known formula [29]

$$\left.\frac{d\ln\tau^{eq}}{d1/T}\right|_{T_g} = -\frac{\partial \ln q_c}{\partial 1/T_g} = \frac{\Delta h*}{R} = mT_g \ln 10. \qquad (12)$$

In this equation, q_c is the experimental cooling rate and T_g is the glass transition temperature determined from the intersection of the enthalpy lines corresponding to the equilibrium liquid and to the glassy states (fictive temperature). The slope of the plot ln τ^{eq} *vs* $1/T_g$ gives the experimental value for $\Delta h^*/R$. From here an experimental fragility can be calculated and their values for the different networks have been also included in Table 5 (the corresponding values of activation energy are also shown). The comparison between experimental and calculated fragilities is quite good for the PEMA networks (difference lower than 10%) and something worse for the PEA and PHEMA (difference around 30%). No clear conclusion can be obtained from the experimental m about the dynamic strength of each network and, therefore, about the influence of each one of the chemical groups that make them different. However it must be taken into account that the experimental calculation of m relies on the value of T_g after several cooling scans at different rates, which means that a single value characterizes a whole thermal history. Besides, some experimental uncertainties appear, on the one hand the fictive temperature T_g calculation needs the accurate identification of the glass curve, which not always easy nor univoquos, on the other hand it must be taken into account that the equipment is not able to follow the programmed cooling scans and from a certain temperature onwards the temperature in the sample diverges from that settled in the program. Besides, we have found no experimental correlation between the width of the distribution of relaxation times β and the fragility index m (see Table 5), as several authors have attempted to obtain [30–31].

Conclusions

The kinetics of the structural relaxation process has been studied for three polymer networks for understanding the influence on this process of the methyl group bonded to the main chain in poly(methacrylates) and the hydroxyl group of the side chain of PHEMA.

The increment of the stiffness of the main chain of poly(methacrylates) with respect to PEA in addition to the shift of the glass transition for around 100 °C towards higher temperatures produces a broadening of the temperature interval of the transition and a increase in the width of the temperature interval in which conformational rearrangements takes place in the glassy state (in the time scale of the 200 min of our structural relaxation experiments). The distribution of relaxation times also broadens as characterised by the decrease of the KWW β parameter.

The hydroxyl group in the side chain of PHEMA adds the possibility of inter- and intra- chain hydrogen bonding. The comparison of the main features of the glass transition and structural relaxation of PHEMA with those of PEMA shows a further increase of glass transition temperature, glass transition temperature width and temperature interval in which the structural relaxation takes place. In addition the behaviour of the network is stronger, in the sense of Angell's classification, than in PEA or PEMA.

To reach these conclusions a detailed analysis of the kinetics of structural relaxation has been performed using a phenomenological model to calculate the relaxation times of the conformational cooperative motions of the polymer chains. The parameters of the model that determine the relaxation times have been determined by curve fitting. In this calculation, it is very important to check to what extent the model equations are able to reproduce the thermograms measured after rather different thermal histories with a single set of model parameters. A procedure to check the consistency of the fitting process and determine the uncertainty of the model parameters has been proposed.

Acknowledgements Support of CICyT project MAT 2001- 2678-C02-01 is acknowledged.

References

1. Davies RO, Jones GO (1953) Adv Phys 2:370
2. Hodge IM (1994) J Non Cryst Solids 169:211
3. Hodge IM (1987) Macromolecules 20:2897
4. Moynihan CT, Macedo PB, Montrose CJ, Gupta PK, DeBolt MA, Dill JF, Dom BE, Drake PW, Easteal AJ, Elterman PB, Moeller RP, Sasabe H (1976) Ann NY Acad Sci 279:15
5. Narayanaswamy OS (1971) J Am Ceram Soc 54:491
6. Kovacs AJ, Aklonis JJ, Hutchinson JM, Ramos AR (1979) J Polym Sci Polym Phys 17:1097
7. Scherer GW (1984) J Am Ceram Soc 67:504
8. Gómez Ribelles JL, Monleón Pradas M (1995) Macromolecules 28:5687
9. Gómez Ribelles JL, Monleón Pradas M, Vidaurre Garayo A, Romero Colomer F, Más Estellés J, Meseguer Dueñas JM (1995) Macromolecules 28:5878
10. Gómez Ribelles JL, Ribes Greus A, Díaz Calleja R (1991) Polymer 31:223
11. Cowie JMG, Ferguson R (1993) Polymer 34:2135
12. Meseguer Dueñas JM, Vidaurre Garayo A, Romero Colomer F, Más Estellés J, Gómez Ribelles JL, Monleón Pradas M (1997) J Polym Sci Polym Phys 35:2201
13. Gómez Ribelles JL, Monleón Pradas M, Vidaurre Garayo A, Romero Colomer F, Más Estellés J, Meseguer Dueñas JM (1995) Polymer 38:963
14. Monserrat S, Gómez Ribelles JL, Meseguer Dueñas JM (1998) Polymer 16:3801
15. Cowie JMG, Harris S, Gómez Ribelles JL, Meseguer JM, Romero F, Torregrosa C (1999) Macromolecules 32:4430
16. Hernández Sánchez F, Meseguer Dueñas JM, Gómez Ribelles JL (2003) J Therm Anal Cal 72:631
17. Andreozzi L, Faetti M, Giordano M, Palazzuoli D, Zulli F (2003) Macromolecules 36:7379
18. Williams G, Watts DC (1970) Trans Faraday Soc 66:80
19. Adam G, Gibbs JH (1965) J Chem Phys 43:139
20. Gibbs JH, DiMarzio EA (1958) J Chem Phys 28:373
21. Saiter A, Oliver JM, Saiter JM, Gómez Ribelles JL (2004) Polymer 45:2743
22. Ho T, Mijović J, (1990) Macromolecules 23:1411
23. Ferry JD (1980) Viscoelastic properties of polymers, 3rd edn. Wiley, New York
24. Angell CA (1991) J Non Cryst Solids 3:131
25. Andreozzi L, Faetti M, Giordano M, Palazzuoli D (2003) J Non Cryst Solids 332:229
26. Hodge IM, Berens AR (1982) Macromolecules 15:762
27. Berens AR, Hodge IM (1982) Macromolecules 15:756
28. Montserrat Ribas SJ (1994) J Polym Sci Polym Phys 32:509
29. Moyniham CT, Easteal AJ, DeBolt MA, Tucker J (1976) J Am Ceram Soc 59:12
30. Böhmer R, Ngai KL, Angell CA, Plazek DJ (1993) J Chem Phys 99:4201
31. Ngai KL, Roland M (1993) Macromolecules 26:6824